This is the final submitted version which was accepted for publication in Magnetic Resonance in Chemistry by Wiley. The published version can be found at https://analyticalsciencejournals.onlinelibrary.wiley.com/doi/10.1002/mrc.5429

The combination of inorganic phosphate and pyrophosphate ^{31}P-NMR for the electrodeless pH determination in the 5-12 range

Paola Carta[1], Mariano Andrea Scorciapino[1,*]

[1]Department of Chemical and Geological Sciences, University of Cagliari, Cittadella di Monserrato, S.P. 8 km 0,700 – I-09042 Monserrato (CA), Italy

[*]Corresponding author: scorciapino@unica.it

Abstract

Potentiometry is the primary pH measurement method, but alternatives are sought beyond glass electrodes operative limitations. In NMR experiments, electrodeless pH sensing is important to track changes along titrations, during chemical reactions or inside compartmentalized environments inaccessible to electrodes, for instance. Although several interesting NMR pH indicators have been already presented, the potential of inorganic phosphate is overlooked, despite its common presence in NMR samples as the buffer main component. Its use for electrodeless pH determination can be expanded by exploiting all its three proton dissociations. This study was aimed at verifying the use of inorganic phosphate ^{31}P chemical shift to sense pH variations, and at exploring the complementary use of pyrophosphate ions to cover a wide pH range. A simple set of equations is presented to utilize both phosphate and pyrophosphate ^{31}P chemical shift in combination for accurate pH determination without a glass electrode over the 5-12 pH range, and without affecting the spectrum of other nuclei. The present study demonstrated an average deviation of 0.09 (maximum < 0.2) pH unit from glass electrode measurements. The trimethylphosphate can be used as a suitable chemical shift reference for both ^{31}P and ^{1}H (also ^{13}C), with its hydrolysis being significant only at pH > 12. The method was also demonstrated by determining the pKa of three distinct molecules in a mixture and by comparing the results to those obtained when the glass electrode was used to measure the pH. The approach shown here can be easily tuned to different experimental conditions.

Keywords: NMR, ^{1}H, ^{31}P, phosphates, electrodeless, pH, pKa, trimethylphosphate hydrolysis kinetics

Introduction

The importance of pH in chemistry is uppermost in many areas, from basic research to cutting-edge applications. Maintaining pH levels is imperative for regulating many chemical reactions in water environment and, especially, for biological processes, as improper pH values can induce protein denaturation, change the electrochemical gradients across membranes and, in general, disrupt cellular functionality. Measuring and controlling pH is paramount for manipulating chemical behavior, as it changes molecular net electric charge and its distribution, thus, intermolecular interactions, reactivity and even the overall stability of chemical systems. Potentiometry is the major technique to measure pH, with even specifically sized glass electrodes commercially available to enter in the typical 5 mm NMR tubes. However, this might not be an option in many instances, so that having one electrodeless way to determine and monitor the pH as a function of time in a NMR experiment is important. Several of such instances are briefly mentioned.

NMR titrations are commonly performed to characterize chemical equilibria.[1–7] To save chemicals, the titration is performed by adding small aliquots of the titrating agent into the NMR tube containing the analyte solution. The insertion of the glass electrode in the NMR tube at each addition, would progressively alter the total volume making the titration largely inaccurate. Unless a very effective buffer can be used, chemical shift variations due to pH changes would overlap with those due to other sources, possibly leading to results misinterpretation.[8] NMR pH-sensing methods must be used to monitor pH evolution in-situ. Furthermore, such methods are needed whenever the solution of interest is compartmentalized and physically inaccessible to a glass electrode, like in the case of lipid vesicles, cubosomes or any other water-filled nanocarrier. In fact, NMR pH indicators are extremely important for biologic in-vitro as well as in-vivo experiments.[9–17] In addition to these practical limitations, there are also known environments where glass electrodes have inherent limitations that can be circumvented by using electrodeless NMR pH-sensing methods, namely, acidic environments containing fluoride,[18] and alkaline environments.[19]

The pH dependence of the NMR chemical shift for a species with an acid-base equilibrium constant in the pH range of interest, can be employed as a NMR pH-indicator. Typically, a fast proton exchange rate is observed on the NMR time scale. The chemical shift vs. pH curve can be fully described with three parameters, as shown by the following equations:[7,20]

$$\chi_{HA}=\frac{[H^+]}{[H^+]+Ka} \quad ; \quad \chi_{A^-}=\frac{Ka}{[H^+]+Ka} \tag{1}$$

$$\delta_{obs} = \chi_{HA}\,\delta_{HA} + \chi_{A^-}\,\delta_{A^-} \quad (2)$$

where, quantities in brackets are molar concentrations, χ_i is the molar fraction of the i-th protonation microspecies, Ka is the deprotonation equilibrium constant, and δ_{obs} is the observed chemical shift. After the three characteristic parameters are determined in the experimental conditions of interest, equation 2 can be solved to determine the unknown pH of a given solution in the $pK_a - 2 < pH < pK_a + 2$ range approximately, through a single chemical shift measurement.

At the pH scale extremes, the main difficulty is the determination of the limiting chemical shift of the fully protonated or deprotonated form, which may be found outside the operative glass electrode pH-range. By exploiting the NMR possibility to measure more than one species simultaneously, the indicator parameters can be accurately determined along a series of selected compounds with sequentially incremented protonation constants. This method has been successfully applied to extend the electrodeless pH determination to highly basic media.[19] By using the same approach, a set of up to six ^{1}H-NMR pH indicators was recently presented to cover the full 2-12 pH range.[21] However, this strategy may suffer from the spectral crowding of both the ^{1}H and the ^{13}C spectra, given by the presence of the indicator molecules themselves together with the analytes. In another very interesting and accurate investigation,[22] the parallel use of both ^{1}H and ^{31}P resonances was put forward. By exploiting the presence of a set of 5 distinct NMR pH indicators, together with multivariate data analysis, high accuracy could be attained over the 0-12 pH range. However, up to 4 and 8 new resonances are added to the ^{1}H and the ^{13}C spectrum, respectively.

Instead of using pH NMR indicators based on fast proton exchange, approaches with slow proton exchanging indicators are possible.[11] However, also this approach can easily lead to spectral crowding.

Ideally, NMR pH determination should come from an active nucleus of enough sensitivity to provide a spectrum with reasonable signal/noise quite fast, thus, also allowing pH monitoring over time with decent time resolution. In addition, the resonances of the pH indicator should not be visible in both ^{1}H and ^{13}C spectra. Beside ^{19}F, whose compounds typically contains carbon and hydrogen atoms, our attention was readily attracted by ^{31}P. In principle, the toxically safe and cheap inorganic phosphate anion would be perfect, since it has as much as three different pKa values, thus covering virtually the entire 2-12 pH range with a single compound. In addition, by virtue of the rapid proton chemical exchange with water, its ^{1}H resonance is typically not observable. Indeed, the tempted application of such strategy to determine the pH

in biological contexts has quite a long story.[9,12–14] Proper calibration of the method has to be preliminarily considered, since the pKa values as well as the limiting chemical shift can change with temperature and ionic strength, but also with the specific nature of the inorganic ions (e.g., Mg^{2+} vs. Na^{+}/K^{+}) and in the presence of other components of the solution (e.g., proteins).

However, the focus of previous studies have been mostly the second proton dissociation constant of the orthophosphoric acid, due to its biologically interesting value close to 7 on the pH scale. The great advantage of using inorganic phosphate is that it is endogenous to virtually all cells. However, the disadvantages connected to the generally low concentration level, the variability with the metabolic state of the cell and the many interactions possible with other components of the intracellular environment, motivated the research for other ^{31}P-NMR pH indicators for in-vivo and in-vitro investigations, such as the 2-deoxyglucose-6-phosphate[23] and several phosphonates.[10,15–17,24] Nevertheless, we believe that the usefulness of inorganic phosphate as NMR pH indicator is underrated, considering also that it is often already present within the sample, as one of the most widely used component of buffers in liquid state NMR investigations. It might be easily and effectively applied in a huge number of NMR investigations, especially if all of the three proton dissociations were exploited. Recently, for instance, even the simultaneous acquisition of both ^{1}H and ^{31}P resonances, with a dual receiver instrumentation, was put forward to follow pH changes during reaction monitoring.[25] This innovative approach of dual reception opened the possibility of in-situ pH measurements and process monitoring at the same time, by determining the pH through ^{31}P chemical shift on one channel, and studying the process kinetics with ^{1}H on the other. The authors made use of the presence of inorganic phosphate within the buffer with success.[25] However, due to the large difference of the three pKa values, some pH ranges cannot be investigated.

In this work, the three proton dissociations of inorganic phosphate were characterized through NMR titration in a simple environment. The limitations of inorganic phosphate have been emphasized and the complementary use of pyrophosphate ions was checked for the first time, as far as we are aware. We present here a simple set of equations to exploit the ^{31}P-NMR resonance of both phosphate and pyrophosphate together for the electrodeless determination of the pH, covering the 5-12 pH range with good accuracy and without any disturbance on either ^{1}H or ^{13}C spectra. We focused on a simple environment, but we kept the sampling of the calibration curves as low as ca. 1 point / pH unit, so that the presented methodology was simple and fast enough to be easily followed to obtain the calibration parameters when different experimental conditions needed to be applied. As an example, this approach was used for the

determination of the pKa values of three distinct molecules in a mixture, and the results were compared to those obtained when the pH was measured with the glass electrode.

Materials and Methods

Potassium dihydrogen phosphate (KH_2PO_4, CAS 7778-77-0), hydrochloric acid (HCl, CAS 7647-01-0), sodium hydroxide (NaOH, CAS 1310-73-2), trimethylphosphate ($C_3H_9PO_4$, CAS 512-56-1), deuterium oxide (D_2O, CAS 7789-20-0), sodium pyrophosphate ($Na_4P_2O_7$, CAS 13472-36-1), acetic acid ($C_2H_4O_2$, CAS 64-19-7), L-histidine ($C_6H_9N_3O_2$, CAS 71-00-1) and 1-aminopentane ($C_5H_{13}N$, CAS 110-58-7) were purchased from Merck (Darmstadt, Germany) with a purity ≥ 95% and used without any further purification. Sterile physiologic solution (NaCl 0.9 $\%_{wt}$) was purchased from Braun (Melsungen, Germany) and used as solvent to prepare all the solutions.

A series of potassium phosphate solutions were prepared by dissolving proper amount of KH_2PO_4 in the NaCl solution supplemented with 10 $\%_{vol}$ D_2O. Final phosphate concentration was 10 mM. The same was performed to prepare a series of solutions of $Na_4P_2O_7$ at 5 mM. A third series of solution was prepared containing both KH_2PO_4 (10 mM) and $Na_4P_2O_7$ (5 mM), together with 5 mM acetic acid, L-histidine and 1-aminopentane. The pH along the three series was corrected by small amounts of concentrated HCl or NaOH to have roughly one data point / pH unit over the 1-13 pH range. The pH was measured at 300 K by potentiometry, with the Metrohm glass electrode 6.0218.010, with built-in Pt-100 temperature sensor, connected to a Metrohm 713 pH-meter calibrated against the three Metrohm reference solutions at pH 4, 7 and 10, respectively. The ionic strength was estimated between 150 and 230 mM by considering the pKa values and the concentration of the differently charged species as a function of the pH.

A volume of 600 µL was loaded into the NMR tube and 1 µL pure trimethylphosphate (TMP) was added right before inserting the tube in the spectrometer. NMR spectra were recorded at 300 K on a Bruker Avance III HD 600 (Bruker, Billerica, MA, USA) operating at a ^{1}H frequency of 600.134 MHz (^{31}P 242.936 MHz). ^{1}H spectra were acquired with 8 transients of the noesypr1d pulse sequence to suppress the water resonance, with 10.9 µs (90°) hard pulses, 2.5 s relaxation delay, 200 ms mixing time, 2.5 s acquisition time and a spectral width of 12.626 kHz. ^{31}P spectra were acquired with 8 transients of power-gated ^{1}H decoupling, with 4.0 µs (30°) hard pulse, 10 s relaxation delay, 3.4 s acquisition time and a spectral width of 9.690 kHz. The TMP resonance was used to calibrate the ppm scale of both ^{1}H (3.81 ppm from DSS,

sodium trimethylsilylpropanesulfonate, Biological Magnetic Resonance Data Bank, entry bmse000774) and ^{31}P (3.80 ppm from 85%$_{wt}$ phosphoric acid).[26]

The chemical shift vs. pH data were analyzed with least squares curve-fitting through Gnuplot (Version 5.2 patchlevel 7). The model equations were obtained by extending equations 1 and 2 to the multi-step proton dissociation equilibria of a given species, H_mA, with m dissociable protons in the pH range of interest:

$$\chi_{H_nA} = \frac{[H^+]^n \beta_{m-n}}{\sum_{j=0}^{m} [H^+]^j \beta_{m-j}} \quad \text{with} \quad 0 \le n \le m \; ; \; \beta_b = \prod_{i=0}^{b} Ka_i \; ; \; Ka_0 = 1 \tag{3}$$

$$\delta_{obs} = \sum_{n=0}^{m} \chi_{H_nA} \; \delta_{H_nA} \tag{4}$$

where, quantities in brackets are molar concentrations, χ_i and δ_i are the molar fraction and the chemical shift of the i-th protonation microspecies, Ka are the deprotonation equilibrium constants, δ_{obs} is the observed chemical shift.

Results and Discussion

The ^{31}P-NMR spectrum of either phosphate or pyrophosphate ions in water solution showed a single resonance, beside the one due to the TMP reference at 3.80 ppm,[26] (Figure 1).

One single resonance at all pH values indicated the fast exchange between the different protonation states of both phosphate and pyrophosphate ions over the entire inspected range. The chemical shift increased with increasing the pH and the trend was monotonic for both phosphate and pyrophosphate. The TMP was selected as chemical shift reference due to its high solubility in water and its single ^{31}P resonance insensitive to pH variations in the 2-12 pH range of interest. In figure 1, at the highest pH values, a low intensity singlet can be observed on the low frequency side of the TMP resonance. This is due to the relatively slow irreversible hydrolysis of TMP at high pH, producing dimethylphosphate (DMP) and methanol, according to the following reaction:

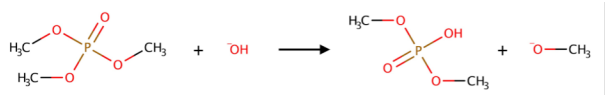

Scheme 1. Trimethylphosphate hydrolysis at high pH to dimethylphosphate and methanol. Methoxide is then protonated by the water solvent by virtue of its large pKa,[27] while dimethylphosphate should be mostly deprotonated.

Formation of methanol was confirmed by the appearance of a singlet at 3.35 ppm in the ^{1}H spectrum, beside the two doublets at 3.81 and 3.57 ppm due to TMP and DMP, respectively. In order to further characterize TMP hydrolysis, we acquired the kinetics at several pH values, by recording the ^{31}P spectrum at regular time intervals. Chemical shift of DMP, differently from TMP, was pH sensitive. Molar fractions were obtained by integrating the TMP and DMP resonances. Results are shown in Figure 2.

Reaction rate depended on hydroxyl ion concentration, such that TMP half-life showed a dramatic increase with decreasing the pH. These experiments have shown that TMP hydrolysis is virtually negligible below pH 12.

Figure 3 shows the curve-fitting analysis of the ^{31}P chemical shift vs. pH of phosphate and pyrophosphate ions, from the stacked plots in Figure 1.

Within the investigated range, three inflection points were clearly observed for both the species, corresponding to three successive proton dissociation equilibrium constants. In the case of phosphate (Figure 3a), inflection points are well separated, whereas in the case of pyrophosphate (Figure 3b), the second and the third inflection points (in the increasing pH order) are quite close. The curve fitting, with equations 3 and 4, allowed to retrieve all the needed parameters to fully describe the chemical shift dependance on the pH. The results are summarized in Table 1. Either the pH-meter readings were considered to build the plots and to perform the curve-fitting, or these were corrected for the isotopic effect as suggested in the literature.[28]

The correction of the pH-meter readings for the isotopic effect resulted to be significant only at basic pH (Figure 3). In particular, it can be observed how the phosphate pKa_3 deviation from the literature data was as large as 0.47 when pH-meter readings were considered, whereas it was reduced to 0.05 by exploiting the isotopic effect correction.[28] All the other pKa values between pH 5 and pH 9, determined on the basis of pH-meter readings, were consistent with the literature data, with a maximum deviation of 0.06. The significant deviation observed at strongly acidic pH for both phosphate and pyrophosphate (0.4 and 0.5, respectively) cannot be ascribed to the isotopic effect on the pH-meter readings, but it is mostly attributable to the rather small chemical shift difference between H_3PO_4 and $H_2PO_4^-$, and between $H_3P_2O_7^-$ and $H_2P_2O_7^{2-}$, respectively. This is reflected by the very short inflection in Figure 3, affecting the determination of the corresponding pKa through the curve-fitting with large inaccuracy and uncertainty (Table 1). Overall, the present results are in agreement with the work by

Rubinson,[48] where it was shown that pH-meter readings do not need any correction for the presence of deuterium in heavy water up to a content of 50%$_{vol}$ and up to a pH of 10.

Thus, for the phosphate, we decided to use the pKa_1, pKa_2, $\delta(H_3PO_4)$, $\delta(H_2PO_4^-)$, and $\delta(HPO_4^{2-})$ obtained with pH-meter readings, and pKa_3 together with the $\delta(PO_4^{3-})$ obtained with the corrected pH values. As far as pyrophosphate is concerned, we kept all the parameters determined with uncorrected pH-meter readings. The corresponding curves can be exploited to determine the pH of a given water solution (same temperature and comparable ionic strength, see Table 1), providing that it contains phosphate or pyrophosphate, by measuring the ^{31}P-NMR chemical shift of these ions instead of using a glass electrode. Figure 4 shows the stacked plot of the ^{1}H-NMR spectra acquired at different pH values, from solutions of a mixture containing equimolar amounts of acetic acid, L-histidine and 1-aminopentane, together with phosphate ions, pyrophosphate ions and TMP (see the Methods).

Resonance assignments are indicated with lowercase letters, as reported beside the Lewis structures on the right-hand side of Figure 4. The two resonances labelled with j and k are due to the product of TMP hydrolysis at strongly basic pH, methanol and DMP, respectively (vide supra), showing no variation of chemical shift as a function of pH in the high pH range. Virtually all resonances of 1-aminopentane, acetic acid and L-histidine changed chemical shift with increasing the pH, by virtue of the progressive change in the protonation state of these molecules. In 1-aminopentane, protons ‘e’ were the most sensitive to the protonation equilibrium of the amino group. As far as the L-histidine is concerned, the proton ‘g’ was the most sensitive to the protonation state of the α-amino group, while proton ‘i’ resulted to be the most sensitive to the protonation state of the imidazole group. Finally, in the case of acetic acid, the only visible resonance was the one due to the protons ‘d’. Figure 5 shows the chemical shift of these selected resonances as a function of pH-meter readings (isotope effect correction was applied to pH $\geq$ 10.0,[28,48] vide supra), together with the curve-fitting (equations 3 and 4) performed to determine the pKa values.

For both acetic acid and 1-aminopentane, a single inflection point could be observed, reflecting the deprotonation equilibrium of the single acid-base site in the molecule. In the case of L-histidine, two inflection points were expected, one at basic pH for the alpha-amino group, and one around pH 6 for the imidazole. The chemical shift vs. pH data of the alpha proton (Figure 5c) allowed to clearly observe the former, whereas the latter was very low. The contrary was observed for the epsilon proton (Figure 5d). The curve-fitting allowed us to determine the pKa values. The latter were determined also by using the electrodeless pH determination through

the measurement of the ^{31}P chemical shift of the same samples for the phosphate and the pyrophosphate ions separately. All the results are reported in the Table 2.

While ^{31}P-NMR chemical shift of the phosphate ions performed well in the neutral pH range, Table 2 shows that inaccuracy increases remarkably both at acidic and basic pH. The deviation of the determined pKa value for the α-amino group of L-histidine was as large as 0.3 pH units. The performance of pyrophosphate ions was comparable at both acidic and neutral pH, but it did not allow to determine pH values larger than about 10. These performances are inherently related to the trend of the ^{31}P chemical shift data vs. pH (Figure 3) which are used to determine the pH itself, as it can be seen from Figure 6.

From Figure 6, it can be seen how accuracy of the proposed electrodeless pH determination dramatically decreased in the plateau regions of the ^{31}P chemical shift vs. pH curve (Figure 3). Pyrophosphate performed better than phosphate at acidic pH, although below pH 5 accuracy was rather low with both the anions. Conversely, above pH 8, the accuracy with the phosphate was higher than with pyrophosphate and, as already mentioned, the determination of pH values larger than about 10 was not even possible with the latter. Overall, neither phosphate nor pyrophosphate ions ^{31}P chemical shift resulted to be acceptably accurate over the entire 2-12 pH range. However, their six different pKa values suggested us to combine their chemical shift vs. pH curves, trying to reduce the plateau regions and improve sensitivity as reported for other cases.[13,14] In principle, a chemical shift curve corresponding to a sufficient number of evenly distributed pKa values should allow accurate electrodeless pH determination over the entire range.

In practice, different linear combinations of the ^{31}P chemical shift vs. pH curves of phosphate and pyrophosphate shown in Figure 3 were calculated as:

$$\delta_{comb}(pH)=c_{phos}\delta_{phos}(pH)+c_{pyro}\delta_{pyro}(pH) \quad (5)$$

where, δ_{phos} and δ_{pyro} are the chemical shift of phosphate and pyrophosphate ions, respectively, and c_{phos} and c_{pyro} are the corresponding coefficients. It is worth noting that every time a new linear combination has to be employed, acquisition of new spectra is not necessary. For each case, the already acquired ^{31}P-NMR spectra corresponding to the ^{1}H stacked plot in Figure 4 were analyzed again, by calculating the selected linear combination of the experimental ^{31}P chemical shift of the phosphate and pyrophosphate ions, in order to determine the pH accordingly. The results of the pKa determination for acetic acid, 1-aminopentane and L-histidine are reported in Table 3.

Overall, a general improvement over the whole pH range was observed, as shown by the deviation between the pKa determined through the electrodeless pH determination and the values obtained with the glass electrode. In Figure 7, the deviation of the pH values is shown for the different linear combinations (equation 5).

By increasing the weight of pyrophosphate in the linear combination, the extremely poor accuracy of phosphate around pH 4 was significantly improved, although a deviation as large as about -0.5 pH units was observed even with $c_{pyro}/c_{phos} = 2$. On the other hand, the accuracy around pH 9 decreased with increasing the weight of pyrophosphate, and at pH 12 it was very low. The best compromise was found with $c_{phos}=1$, and by decreasing c_{pyro} to 0.25. Overall, this combination resulted to be the most accurate one over the full pH range between 5 and 12, with deviation from the glass electrode measurements exceeding 0.1 only above pH 10, and maximum deviation below 0.2 pH units. Nevertheless, the steeply large deviation around pH 4 remained. Such inaccuracy of the proposed electrodeless determination is basically due to the short inflection at acidic pH for both phosphate and pyrophosphate ^{31}P chemical shift vs. pH (Figure 3). A third phosphorus compound with suitable pKa must be included to cover acidic environments. In the work of Szakács et al., the ^{31}P resonance of inorganic phosphate was proposed together with the ^{1}H resonances from other 4 simple organic molecules to cover the entire 0-12 pH range.[22] By exploiting multiple titration curves at a time, high accuracy was attained (with ca. 3 data points / pH unit). Overall, the accuracy we obtained in the 5-12 pH range was slightly lower. However, the presented approach does not add any resonance in either the ^{1}H and the ^{13}C spectrum (beside the TMP), it required only ca. 1 data point / pH unit and it did not involve multiple titration curves or multivariate data analysis.

Conclusions

The present investigation demonstrated how pH can be easily determined in the 5-12 pH range without making use of a glass electrode with an average accuracy of 0.09 (maximum deviation < 0.2) pH units. Providing that the solution of interest (10%$_{vol}$ D_2O and ionic strength of 150-200 mM) contains phosphate and pyrophosphate ions, together with TMP as chemical shift reference, experimental ^{31}P chemical shift values can be exploited according to the following equations:

$$\delta(\mathrm{pH})=\delta_{phos}(\mathrm{pH})+0.25\cdot\delta_{pyro}(\mathrm{pH})$$

$$\delta_{\text{phos}}(\text{pH}) = \frac{0.62 \cdot 10^{-3 \cdot pH} + 0.86 \cdot 10^{-2 \cdot pH - 2.2} + 3.34 \cdot 10^{-pH - 8.96} + 5.99 \cdot 10^{-20.61}}{10^{-3 \cdot pH} + 10^{-2 \cdot pH - 2.2} + 10^{-pH - 8.96} + 10^{-20.61}}$$

$$\delta_{\text{pyro}}(\text{pH}) = \frac{-10.23 \cdot 10^{-3 \cdot pH} - 9.72 \cdot 10^{-2 \cdot pH - 2.3} - 6.63 \cdot 10^{-pH - 8.23} - 5.30 \cdot 10^{-16.49}}{10^{-3 \cdot pH} + 10^{-2 \cdot pH - 2.3} + 10^{-pH - 8.23} + 10^{-16.49}}$$

These equations can be used in the simple environment employed in this work, while a new calibration is needed if different ions are present, especially divalent Mg^{2+} or Ca^{2+}, or in the presence of proteins or other components. However, the presented methodology is simple (calibration curves have been sampled with ca. 1 point / pH unit) and can be easily tuned. TMP is suitable as chemical shift reference for both ^{31}P (3.80 ppm), ^{1}H (3.81 ppm), as well as for ^{13}C (57.72 ppm from DSS, Biological Magnetic Resonance Data Bank, entry bmse000774). TMP hydrolysis was shown to be important only at high pH (>12), where it dissociates to DMP and methanol (at pH 12 TMP half-life is about 90 hours). The presented electrodeless approach to pH determination can be used in a very large number of NMR investigations and extend the applicability of the $^{31}P/^{1}H$ dual reception strategy recently proposed to measure the pH in the nmr tube while monitoring the evolution of the system at the same time.[25] Studies with liposomes or other compartmentalized model systems are also possible, providing that phosphate and pyrophosphate are present on both sides. However, in the case of intact cells, for instance, membrane permeability to the two inorganic ions must be preliminarily checked.

Acknowledgements

Dr. Sandrina Lampis and the CeSAR (Centro Servizi di Ateneo per la Ricerca) of the University of Cagliari are acknowledged for the NMR measurements. Dr. Rosita Cappai (University of Sassari) is acknowledged for the fruitful discussions.

References

[1] P. Thordarson, *Chem. Soc. Rev.* **2011**, *40*, 1305.
[2] A. J. Lowe, F. M. Pfeffer, P. Thordarson, *Supramolecular Chemistry* **2012**, *24*, 585.
[3] M. J. Hynes, *J. Chem. Soc., Dalton Trans.* **1993**, 311.
[4] W. Becker, K. C. Bhattiprolu, N. Gubensäk, K. Zangger, *ChemPhysChem* **2018**, *19*, 1.
[5] A. Garau, G. Picci, A. Bencini, C. Caltagirone, L. Conti, V. Lippolis, P. Paoli, G. M. Romano, P. Rossi, M. A. Scorciapino, *Dalton Trans.* **2022**, *51*, 8733.
[6] M. A. Scorciapino, G. Malloci, I. Serra, S. Milenkovic, L. Moynié, J. H. Naismith, E. Desarbre, M. G. P. Page, M. Ceccarelli, *Biometals* **2019**, DOI 10.1007/s10534-018-00166-0.
[7] J. Bezençon, M. B. Wittwer, B. Cutting, M. Smieško, B. Wagner, M. Kansy, B. Ernst, *Journal of Pharmaceutical and Biomedical Analysis* **2014**, *93*, 147.

[8] A. K. Pandey, C. R. Buchholz, N. Nathan Kochen, W. C. K. Pomerantz, A. R. Braun, J. N. Sachs, *ACS Chem. Neurosci.* **2023**, *14*, 800.
[9] Y. Seo, M. Murakami, H. Watari, Y. Imai, K. Yoshizaki, H. Nishikawa, T. Morimoto, *J Biochem* **1983**, *94*, 729.
[10] M. DeFronzo, R. J. Gillies, *Journal of Biological Chemistry* **1987**, *262*, 11032.
[11] L. H. Perruchoud, M. D. Jones, A. Sutrisno, D. B. Zamble, A. J. Simpson, X. -a Zhang, *Chem. Sci.* **2015**, *6*, 6305.
[12] R. Jayasundar, L. D. Hall, N. M. Bleehen, *NMR in Biomedicine* **1992**, *5*, 360.
[13] W. J. Thoma, J. G. Steiert, R. L. Crawford, K. Ugurbil, *Biochemical and Biophysical Research Communications* **1986**, *138*, 1106.
[14] R. J. Labotka, R. A. Kleps, *Biochemistry* **n.d.**, *22*, 6089.
[15] S. Pietri, S. Martel, M. Culcasi, M.-C. Delmas-Beauvieux, P. Canioni, J.-L. Gallis, *Journal of Biological Chemistry* **2001**, *276*, 1750.
[16] S. Pietri, M. Miollan, S. Martel, F. Le Moigne, B. Blaive, M. Culcasi, *Journal of Biological Chemistry* **2000**, *275*, 19505.
[17] M. J. Fisher, P. F. Dillon, *Circ Res* **1987**, *60*, 472.
[18] J. B. Gerken, *Journal of Fluorine Chemistry* **2011**, *132*, 68.
[19] G. Orgován, B. Noszál, *Journal of Pharmaceutical and Biomedical Analysis* **2011**, *54*, 958.
[20] A. D. Gift, S. M. Stewart, P. Kwete Bokashanga, *J. Chem. Educ.* **2012**, *89*, 1458.
[21] G. Orgován, B. Noszál, *Anal. Chem.* **2018**, *90*, 12075.
[22] Z. Szakács, G. Hägele, R. Tyka, *Analytica Chimica Acta* **2004**, *522*, 247.
[23] G. E. Soto, Z. Zhu, J. L. Evelhoch, J. J. Ackerman, *Magn Reson Med* **1996**, *36*, 698.
[24] M. D. Reily, L. C. Robosky, M. L. Manning, A. Butler, J. D. Baker, R. T. Winters, *J. Am. Chem. Soc.* **2006**, *128*, 12360.
[25] N. Cox, R. Kuemmerle, P. Millard, E. Cahoreau, J.-M. François, J.-L. Parrou, G. Lippens, *Anal. Chem.* **2019**, *91*, 3959.
[26] R. Streck, A. J. Barnes, *Spectrochimica Acta Part A: Molecular and Biomolecular Spectroscopy* **1999**, *55*, 1049.
[27] P. Ballinger, F. A. Long, *J. Am. Chem. Soc.* **1960**, *82*, 795.
[28] A. Krężel, W. Bal, *Journal of Inorganic Biochemistry* **2004**, *98*, 161.
[29] T. Kiss, E. Kiss, G. Micera, D. Sanna, *Inorganica Chimica Acta* **1998**, *283*, 202.
[30] K. Atkári, T. Kiss, R. Bertani, R. B. Martin, *Inorg Chem* **1996**, *35*, 7089.
[31] A. Saha, N. Saha, L. -n. Ji, J. Zhao, F. Gregáň, S. A. A. Sajadi, B. Song, H. Sigel, *JBIC* **1996**, *1*, 231.
[32] S. Głąb, M. Maj-Zurawska, P. łukomski, A. Hulanicki, A. Lewenstam, *Analytica Chimica Acta* **1993**, *273*, 493.
[33] D. R. Turner, M. M. Correia dos Santos, P. Coutinho, M. de Lurdes Gonçalves, S. Knox, *Analytica Chimica Acta* **1992**, *258*, 259.
[34] P. G. Daniele, A. De Robertis, C. De Stefano, A. Gianguzza, S. Sammartano, *J Solution Chem* **1991**, *20*, 495.
[35] R. E. Mesmer, C. F. Baes, *J Solution Chem* **1974**, *3*, 307.
[36] J. Martinez Calatayud, P. Campins Falcó, R. Micó Albert, *Analyst* **1987**, *112*, 1063.
[37] G. E. Jackson, K. V. V. Voyi, *South African Journal of Chemistry* **1988**, *41*, 17.
[38] P. W. Linder, J. C. Little, *Talanta* **1985**, *32*, 83.
[39] D. Banerjea, T. A. Kaden, H. Sigel, *Inorg. Chem.* **1981**, *20*, 2586.
[40] A. Vacca, A. Sabatini, L. Bologni, *J. Chem. Soc., Dalton Trans.* **1981**, 1246.
[41] O. Mäkitie, V. Konttinen, *Acta Chemica Scandinavica* **1969**, *23*, 1459.
[42] P. Buglyó, T. Kiss, E. Alberico, G. Micera, D. Dewaele, *Journal of Coordination Chemistry* **1995**, *36*, 105.

[43] P. E. Jurek, A. E. Martell, R. J. Motekaitis, R. D. Hancock, *Inorg. Chem.* **1995**, *34*, 1823.
[44] Q. Lu, R. J. Motekaitis, J. J. Reibenspies, A. E. Martell, *Inorg. Chem.* **1995**, *34*, 4958.
[45] C. D. Stefano, C. Foti, O. Giuffrè, *Journal of Chemical Research, Synopses* **1998**, *0*, 480.
[46] J. R. Duffield, D. R. Williams, I. Kron, *Polyhedron* **1991**, *10*, 377.
[47] A. Craggs, G. J. Moody, J. D. R. Thomas, *Analyst* **1979**, *104*, 412.
[48] K. A. Rubinson, *Anal. Methods* **2017**, *9*, 2744.
[49] H. Fukada, K. Takahashi, *Proteins* **1998**, *33*, 159.
[50] N. C. Li, B. E. Doody, J. M. White, *J. Am. Chem. Soc.* **1957**, *79*, 5859.
[51] R. S. Asquith, P. Carthew, H. D. Hanna, M. S. Otterburn, *Journal of the Society of Dyers and Colourists* **1974**, *90*, 357.
[52] M. I. A. Ferra, J. R. Graça, A. M. M. Marques, *J. Chem. Eng. Data* **2011**, *56*, 3673.
[53] A. Chakravorty, F. A. Cotton, *J. Phys. Chem.* **1963**, *67*, 2878.
[54] S. Ganesan, V. Sudhakaran Menon, M. V. Rajendran, R. K. Raman, A. Alagumalai, A. Krishnamoorthy, *Materials Science in Semiconductor Processing* **2024**, *169*, 107904.
[55] H. S. O. P. Harned, F. C. Hickey, *J. Am. Chem. Soc.* **1937**, *59*, 1284.
[56] J. L. Meyer, J. E. Jr. Bauman, *J. Am. Chem. Soc.* **1970**, *92*, 4210.
[57] D. R. Lide, *CRC Handbook of Chemistry and Physics*, Taylor And Francis, Boca Raton (FL) - U.S.A., **2007**.

Table 1. Results from the curve-fitting (equations 3 and 4) of the data shown in Figure 3. Chemical shift of the ^{31}P resonance[a] from the different protonation states of both phosphate and pyrophosphate ions. The proton dissociation equilibrium constant determined in this work are compared with data from the literature obtained with potentiometry. Relevant conditions of the medium used in this work: ionic strength 0.15-0.20 M, temperature 300 K, D_2O 10%$_{vol}$.

Phosphate							
	pKa_1	pKa_2	pKa_3	$\delta(H_3PO_4)$ [ppm]	$\delta(H_2PO_4^-)$ [ppm]	$\delta(HPO_4^{2-})$ [ppm]	$\delta(PO_4^{3-})$ [ppm]
This work[b]	2.2±0.3	6.76±0.02	12.07±0.03	0.62±0.05	0.86±0.01	3.34±0.01	5.94±0.03
This work[c]	2.2±0.4	6.65±0.02	11.65±0.03	0.59±0.08	0.83±0.02	3.33±0.01	5.99±0.03
Literature data							
	pKa_1	pKa_2	pKa_3	medium	Concentration [M]	Temperature [K]	
Ref.[9]		6.82		KCl	0.15	297	
Ref.[9]		6.79		KCl	0.15	297	
Ref.[9]		6.73		NaCl	0.15	297	
Ref.[9]		6.68		KCl + $MgCl_2$	0.135 + 0.05	297	
Ref.[9]		6.70		KCl + $MgCl_2$	0.11 + 0.01	297	
Ref.[9]		6.70		KCl + $CaCl_2$	0.135 + 0.05	297	
Ref.[9]		6.71		KCl + $CaCl_2$	0.11 + 0.01	297	
Ref.[29]	1.83	6.63	11.46	KCl	0.2	298	
Ref.[30]	1.86	6.63	11.48	KCl	0.2	298	
Ref.[31]	1.8	6.75	11.68	$NaNO_3$	0.1	298	
Ref.[32]	2.42	7.28		NaCl	0.15	298	
Ref.[33]	1.93	6.79	11.69	KCl	0.1	298	
Ref.[34]	1.9	6.69	11.56	KCl	0.16	298	
Ref.[35]		7.044	11.886	KCl	0.1	298	
Ref.[36]		6.70	11.71	NaCl	0.25	298	
Ref.[37]	1.20	6.51	11.8	NaCl	0.15	298	
Ref.[38]	1.68	6.40	11.18	KCl	0.2	298	
Ref.[39]		6.73		$NaNO_3$	0.1	298	
Ref.[40]	1.843	6.635	11.545	NaCl	0.1	298	
Ref.[41]		6.76		KCl	0.1	298	
	1.8±0.3	6.7±0.2	11.6±0.2	Average and Standard Deviation			

Pyrophosphate							
	pKa_2	pKa_3	pKa_4	$\delta(H_3P_2O_7^-)$ [ppm]	$\delta(H_2P_2O_7^{2-})$ [ppm]	$\delta(HP_2O_7^{3-})$ [ppm]	$\delta(P_2O_7^{4-})$ [ppm]
This work[b]	2.3±0.2	5.93±0.04	8.26±0.08	-10.23±0.06	-9.72±0.05	-6.63±0.07	-5.30±0.02
This work[c]	2.4±0.2	5.95±0.04	8.26±0.08	-10.27±0.06	-9.74±0.05	-6.50±0.07	-5.24±0.02
Literature data							
	pKa_2	pKa_3	pKa_4	medium	Concentration [M]	Temperature [K]	
Ref.[30]	1.67	5.88	8.23	KCl	0.2	298	
Ref.[42]	1.66	5.88	8.25	KCl	0.2	298	
Ref.[43]	1.8	5.95	8.4	KCl	0.1	298	
Ref.[44]	2.07	6.09	8.55	KCl	0.1	298	
Ref.[45]	1.66	5.69	7.84	NaCl	0.25	298	
Ref.[45]	1.65	5.83	8.06	KCl	0.25	298	

Ref.[46]	1.756	5.872	8.138	NaCl	0.15	298
Ref.[47]		5.79	8.05	NaCl	0.1	298
Ref.[37]		6.34	8.67	NaCl	0.15	298
	1.8±0.1	5.9±0.2	8.2±0.2	Average and Standard Deviation		

[a]Chemical shift scale was calibrated with TMP at 3.80 ppm[26]

[b]pH-meter readings

[c]pH corrected for the isotopic effect[28]

Table 2. Results of the curve fitting with equations 3 and 4 of the chemical shift vs. pH for selected ^{1}H-NMR resonances of acetic acid (C(2)H$_3$), L-histidine (Hα and Hε) and 1-aminopentane (C(1)H$_2$) in a mixture with also phosphate and pyrophosphate ions, and TMP as a reference (both for ^{1}H and ^{31}P). Proton dissociation equilibrium constants from the literature obtained with potentiometry at comparable temperature and ionic strength are reported for comparison.

pH determination	Acetic acid (carboxylic group)	L-histidine (imidazole group)	L-histidine (α-amino group)	1-aminopentane (amino group)
Glass electrode	4.56±0.01	6.24±0.02	9.44±0.04	10.84±0.01
^{31}P phosphate	4.4±0.2	6.28±0.04	9.74±0.08	10.97±0.02
^{31}P pyrophosphate	4.4±0.1	6.20±0.02	indeterminable	indeterminable
		Deviations		
^{31}P phosphate	-0.16	0.04	0.30	0.13
^{31}P pyrophosphate	-0.16	-0.04	indeterminable	indeterminable
		Literature data		
	4.62[49]	6.17[50]	9.20[50]	10.63[51]a
	4.65[52]	6.08[53]	9.17[53]	10.6[54]a
	4.54[55]	6.17[56]	9.21[56]	10.63[57]a

[a]Ionic strength not reported.

Table 3. Results of the curve fitting with equation 3 and 4 of the chemical shift vs. pH for selected ^{1}H-NMR resonances of acetic acid (C(2)H$_3$), L-histidine (Hα and Hε) and 1-aminopentane (C(1)H$_2$) in a mixture with also phosphate and pyrophosphate ions, and TMP as a reference (both for ^{1}H and ^{31}P). The pH was determined without potentiometry but using the experimental ^{31}P chemical shift of both phosphate and pyrophosphate ions in different linear combinations (equation 5).

Combination coefficients	Acetic acid (carboxylic group)	L-histidine (imidazole group)	L-histidine (α-amino group)	1-aminopentane (amino group)
$c_{phos} = 1$ $c_{pyro} = 1$	4.5±0.1	6.22±0.03	9.13±0.02	10.94±0.02
$c_{phos} = 1$ $c_{pyro} = 2$	4.5±0.1	6.21±0.02	9.09±0.02	10.90±0.02
$c_{phos} = 1$ $c_{pyro} = 0.5$	4.5±0.2	6.23±0.03	9.22±0.01	10.95±0.02
$c_{phos} = 1$ $c_{pyro} = 0.25$	4.5±0.2	6.25±0.03	9.36±0.01	10.97±0.02
		Deviations[a]		
$c_{phos} = 1$ $c_{pyro} = 1$	-0.06	-0.02	-0.31	0.10
$c_{phos} = 1$ $c_{pyro} = 2$	-0.06	-0.03	-0.35	0.06
$c_{phos} = 1$ $c_{pyro} = 0.5$	-0.06	-0.01	-0.22	0.11
$c_{phos} = 1$ $c_{pyro} = 0.25$	-0.06	0.01	-0.08	0.13
^{31}P phosphate	-0.16	0.04	0.30	0.13
^{31}P pyrophosphate	-0.16	-0.04	indeterminable	indeterminable

[a]Deviation is calculated with respect to the glass electrode measurement (Table 2).